B: Liquids, Chemical and Dynamical Processes in Solution, Spectroscopy in Solution

Sum-Frequency Signals in 2D-Terahertz-Terahertz-Raman Spectroscopy

Griffin Mead, Haw-Wei Lin, Ioan-Bogdan Magdau, Thomas Francis Miller, and Geoffrey A. Blake

J. Phys. Chem. B, **Just Accepted Manuscript** • DOI: 10.1021/acs.jpcb.0c07935 • Publication Date (Web): 08 Sep 2020

Sum-Frequency Signals in 2D-Terahertz-Terahertz-Raman Spectroscopy

Griffin Mead,[†] Haw-Wei Lin,[†] Ioan-Bogdan Magdău,[†] Thomas F. Miller III,[†] and Geoffrey A. Blake*[,†,‡]

†*Division of Chemistry & Chemical Engineering, California Institute of Technology, Pasadena, California 91125, United States*
‡*Division of Geological & Planetary Sciences, California Institute of Technology, Pasadena, California 91125, United States*

E-mail: gab@gps.caltech.edu

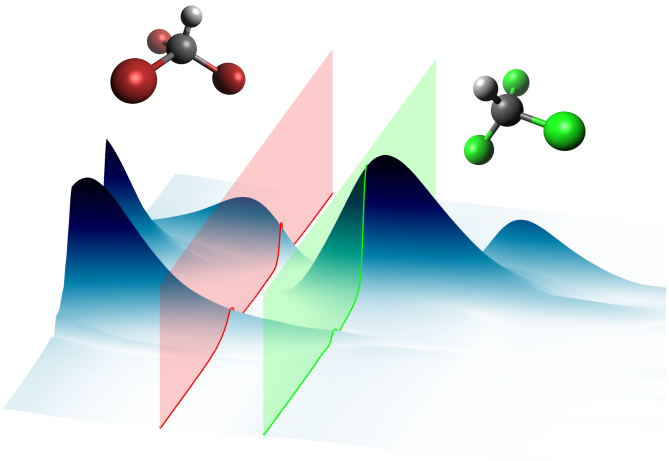

Figure 1: Table of contents figure

Abstract

We demonstrate that halogenated methane 2D-Terahertz Terahertz Raman (2D-TTR) spectra are determined by the complicated structure of the instrument response function (IRF) along ω_1 and by the molecular coherences along ω_2. Experimental improvements have helped increase the resolution and dynamic range of the measurements, including accurate THz pulse shape characterization. Sum-frequency excitations convolved with the IRF are found to quantitatively reproduce the 2D-TTR signal. A new Reduced Density Matrix model which incorporates sum-frequency pathways, with linear and harmonic operators fully supports this (re)interpretation of the 2D-TTR spectra.

Main text

Observing interactions within the low-frequency, thermally populated continuum of bath states is critical to developing a molecular understanding of liquid dynamics at room temperature. This energy regime is predominantly characterized by broad inter-molecular modes with short coherence times (∼100s fs) which complicate the measurement and interpretation of potential energy, dipole and polarizability surfaces. One exception to this general observation are the intra-molecular vibrational modes of the halogenated methane (HM) family of liquids, whose well-defined coherent vibrational signals have long been observed in optical Kerr effect (OKE) experiments.[1,2]

Multidimensional time-resolved spectroscopy methods seek to disentangle **the molecular processes underlying the low-frequency spectral features** by introducing an additional time delay which separates dynamics along a second axis. The 5th order Raman

technique[3] extends OKE to two dimensions and provides information on electrical and mechanical anharmonicities of the liquid, but practical implementation of this method is quite challenging.[4,5] A trio of 3^{rd} order terahertz-Raman hybrid spectroscopies have been proposed as alternatives to 5^{th} order Raman spectroscopy that avoid some technical challenges inherent to 5^{th} order spectroscopy.[6–11] However, new challenges emerge in the hybrid techniques, especially compared to the more common 2D-infrared (2D-IR) spectroscopy, **in which molecular coherences and population states are manipulated through electric dipole-allowed transitions**. First, there are no commercially available dispersive THz spectrometers with adequate sensitivity to directly detect the emitted THz signal in THz-Raman-THz (2D-TRT) and Raman-THz-THz (2D-RTT) measurements. Instead, the 2D-TRT/RTT techniques have used time-domain electro-optic sampling to capture the faint THz emission.[12] 2D-TTR avoids this step by using a Raman probe pulse which generates an easily detected near-IR signal photon.

The Raman probe does mean, however, that the resonant excitation of coherences with the THz pulses in TTR experiments is driven by nonlinearities in the transition dipole surface, as we outline below. Further, in all the cases of hybrid THz-Raman spectroscopies, the poorly defined wave vector **resulting from sub-cycle THz pulses** precludes a phase-matching box-CARS style geometry that could be used to discriminate between signals originating from different quantum mechanical coherence pathways.

With 2D-TTR spectroscopy, complex spectra have been observed in several halogenated methane (HM) liquids, and were interpreted as signatures of coherent energy transfer pathways between intra-molecular vibrational modes.[13–16]. **In this work, we present a thorough** re-investigation of two HM liquids – bromoform ($CHBr_3$) and chloroform ($CHCl_3$) – which casts doubt on this original interpretation. Our new investigation is enabled by the development of a single-shot 2D-TTR spectrometer[17] which records tens of picoseconds of molecular dynamics in a single acquisition. From the order of magnitude speed-up, the new technique provides substantially higher signal-to-noise data which has allowed a much larger region of the molecular response to be measured, and at finer resolution.

We demonstrate through experiment, models, and theoretical simulations that the features observed in the HM 2D-TTR spectra arise from convolutions between the instrument response function (IRF) and linear interactions with the molecular polarizability operator Π. This interaction requires a scattering with two instantaneous THz photons, and is therefore referred to throughout the text as a sum-frequency (SF) excitation process. (Recent theoretical and experimental works have also observed efficient phonon excitation through the same linear-Π interaction with two THz field interactions.[18–20]) Resonant nonlinear interactions with the transition dipole operator M, while also in principal weakly allowed, are not seen.

We begin by re-examining the relative importance of the M (resonant) and Π (sum-frequency) excitation pathways in HM vibrational modes. Ladder diagrams in Fig. 2 illustrate the two competing pathways as well as the OKE process. **While analogous to SF-TKE, OKE measurements involve virtual states that are typically far removed from either electronic or fundamental vibrational states. SF-TKE processes, in contrast, involve photons that can directly excite intermolecular degrees of freedom in the liquid.**

In order to observe the desired nonlinear THz signal, the resonant pathway must have a larger or (at least) comparable magnitude with the sum-frequency pathway. This is a difficult condition to satisfy in HMs since the resonant process is nonlinear with respect to M while the sum-frequency pathway is linear in Π.

Sum-frequency and resonant excitation pathways have distinct t_1 responses. A clear sign of resonant M interactions is a prolonged vibrational response along t_1 which arises from the generation of a vibrational coherence during the first THz field interaction. **From 2D-TTR measurements, molecular coherences ex-**

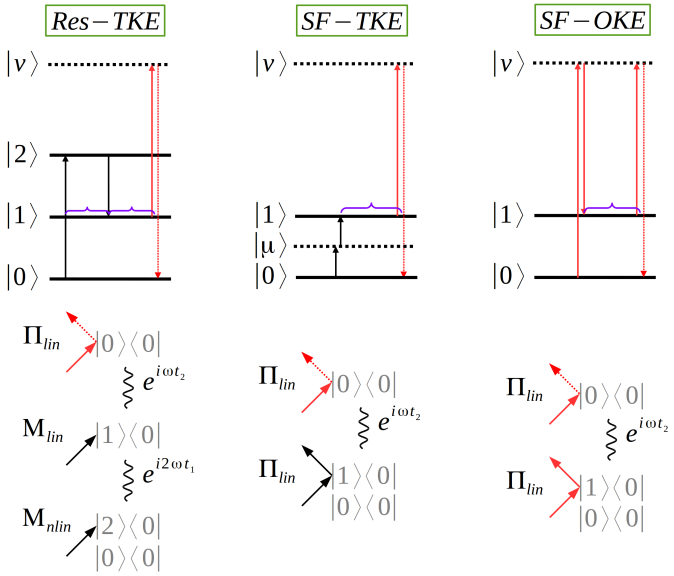

Figure 2: A resonant TTR signal requires dipole nonlinearities to excite a vibrational coherence – a representative process is depicted in the Res-TKE (resonant THz Kerr Effect) ladder and Feynman diagrams. In contrast, a sum-frequency excited molecular coherence is produced via interactions linear in the polarizability operator. The virtual state in SF-TKE is short-lived, thus the signal is highly dependent upon overlap between the two pump pulses. The familiar optical Kerr effect (SF-OKE) illustrates the similarities with SF-TKE.

tending in excess of 5 ps along t_2 have been observed in HMs[14], suggesting a resonant signal should have a commensurate lifetime along t_1. In contrast, sum-frequency excitation cannot directly generate coherent states through a single field interaction, but requires two instantaneous interactions. In this case, the extent of a molecular response along t_1 will be determined by the duration of temporal overlap of the two THz electric field waveforms.

In Fig. 3 time-domain bromoform and chloroform measurements recorded under identical experimental conditions are shown. The key observation is that while the t_2 response is long-lived, that along t_1 never extends past the region of THz field overlap. Both bromoform's and chloroform's vibrational coherent responses are therefore far more consistent with a SF excitation mechanism than a resonant process.

The different bandwidth requirements of the two processes provides a second argument supporting SF excitation as the dominant pathway. In both SF and resonant 2D-TTR pathways, a vibrational mode must begin and end the measurement in a population state. In addition, the Raman probe interaction only changes the vibrational quanta by ± 1. If a M non-linearity is present, one of the THz field interactions must produce either a zero-quanta or two-quanta excitation, or bandwidths spanning $\geq 2\omega$ in the latter case.[21] (No evidence for zero-quanta transitions have been observed.) Again, this is quite different from 2D-IR spectroscopies. SF excitation, on the other hand, progresses with a bandwidth $\approx \omega/2$. The experimental THz field bandwidth spans 1-5 THz, and therefore the 2D-TTR experiment lacks the necessary frequency content to produce vibrational coherences arising from M non-linearities in the molecular Hamiltonian.

Given that sum-frequency excitation is the predominant source of the signals observed in 2D-TTR spectroscopy of HMs, a key mystery becomes how this mechanism, whose instantaneous nature precludes separating the two THz field interactions in time, can nonetheless produce a signal which varies along t_1? We interrogate the origins of this complex t_1 response by considering how the observed signal $S(t_1, t_2)$ depends upon the IRF $I(t_1, t_2)$ (Eq. 1). In a 2D-TTR experiment, two orthogonally polarized THz fields ($\vec{x}, \vec{y}$ in the lab frame) create a birefringent response within the room-temperature HM liquid sample. A $\vec{x}$ polarized Raman probe scatters off this birefringence, producing a $\vec{y}$ polarized signal field that is selectively isolated through an analyzing polarizer and differential chopping. The 2D-TTR signal is proportional to the anisotropic third-order molecular response function $R^{(3)}_{xyxy}(t_1, t_2)$, and contains information on the molecular orientational and vibrational correlation functions of the system. During the measurement process, this response is inevitably convolved with the experimental IRF, which in 2D-TTR is determined by the product of the two THz electric fields.

$$S(t_1, t_2) = I(t_1, t_2) \circledast R^{(3)}_{xyxy}(t_1, t_2) \qquad (1)$$

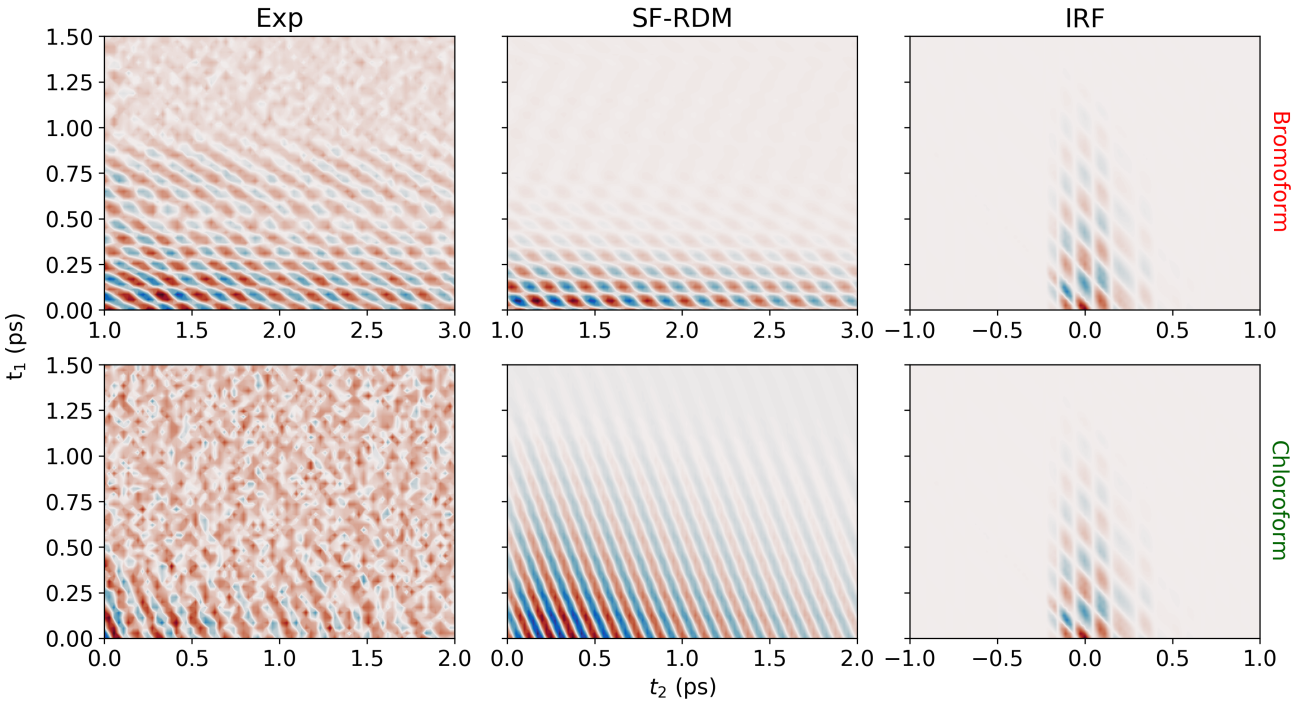

Figure 3: Top and bottom rows compare the experimental (Exp) bromoform and chloroform time-domain data to the SF-RDM models. The calculated IRF, whose THz electric fields are used as inputs to the SF-RDM model, is shown for reference (right column). Identical pulse shapes and IRFs are used for both SF-RDM models of bromoform and chloroform.

Through the convolution theorem, the time-domain convolution becomes a multiplication between the IRF spectral power and the HM molecular response function upon transformation to the frequency domain.

$$\tilde{S}(\omega_1, \omega_2) = \tilde{I}(\omega_1, \omega_2) \cdot \tilde{R}^{(3)}_{xyxy}(\omega_1, \omega_2) \qquad (2)$$

We study the impact of IRF convolution in two ways. First, we generate a time-domain model IRF (Fig. 3) using model THz field profiles (Fig. 6) that closely resemble experimental pulse shapes (see SI for details). An instantaneous SF process gives a molecular response which is a delta function in the time-domain (t_1) and a flat response in the corresponding frequency domain ($\boldsymbol{\omega_1}$). In 2D-TTR, this amounts to a flat response along the ω_1 axis, and a delta functions along the ω_2 axis centered at the eigenmode frequencies of the molecular sample. Multiplication of this molecular response with the IRF yields the final measured signal. This results in simply selecting a slice of the IRF along ω_1 at the eigenmode frequency. Using this simple model we find excellent agreement with the experimental spectra.

Second, we use the same THz field profiles that produce the IRF model as inputs to RDM simulations that consider sum-frequency excitation processes (SF-RDM). Again, we find near-quantitative agreement between the experimental data and theoretical simulations. Critically, no electrical or mechanical non-linearities are required to reach excellent agreement between the data and the IRF model/RDM simulations. The SF-RDM results precisely reproduce the experimental time-domain (Fig. 3) and frequency-domain (Fig. 4) responses, substantiating the claim that SF processes dominate the 2D-TTR response of HMs.

The agreement between experiment, SF-RDM, and model IRF are shown in Fig. 5. While bromoform and chloroform have different intramolecular vibrational energies, we reproduce

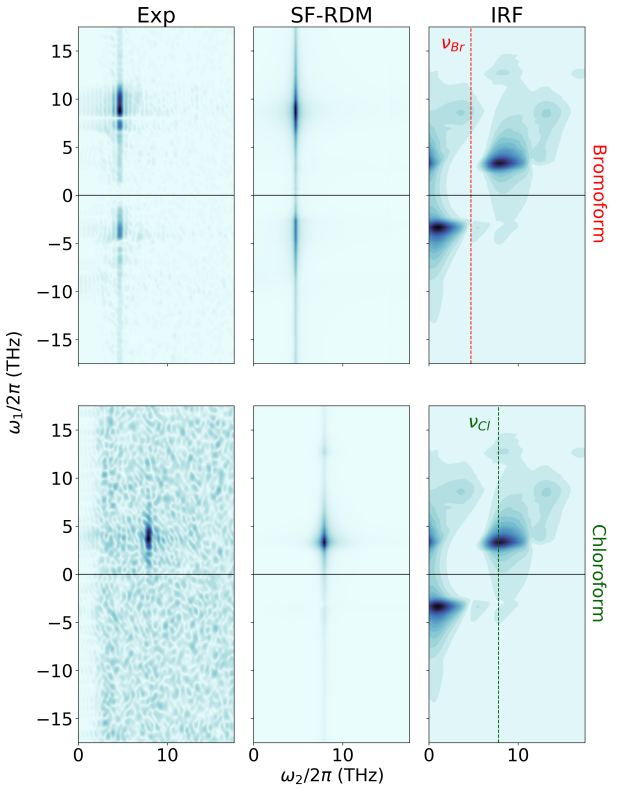

Figure 4: Top and bottom rows compare the experimental (Exp) bromoform and chloroform frequency-domain data to the SF-RDM model. The calculated IRF is shown for reference with vertical lines indicating where each HMs intramolecular vibrational mode samples the IRF. Note that the experimental and SF-RDM spectra are well matched, and arise from sampling the same IRF at different ω_2 frequencies.

both spectra by slicing the same model IRF at their respective eigenmode frequencies along ω_2. Crucially, this model mimics the non-specific sum-frequency excitation of vibrational coherences by the THz electric field. Unlike previous interpretations, here we do not invoke Feynman diagram pathways involving multi-quanta transitions between several vibrational modes; instead, the experimental IRF filtered through a single SF excitation pathway explains the data. That a two-quanta sum-frequency excitation pathway is predominantly responsible for vibrational coherences observed in 2D-TTR is also supported by estimations of chloroform and bromoform's transition dipole moments. **From THz-TDS measurements and FT-IR literature, the bromoform and chloroform E mode's molar extinction coefficients were $\epsilon \approx 1 M^{-1} cm^{-1}$, suggestive of a vanishingly small transition dipole moment.**[22] As a result, it would be very difficult to observe resonant excitation of these HM modes, even in the absence of interfering SF pathways. For comparison, 2D-IR spectroscopy on proteins is often performed by resonantly pumping the amide I stretch at $\sim$ 50 THz, which have ϵ $\sim$200-400 $M^{-1}cm^{-1}$. Not only are these oscillators intrinsically orders of magnitude stronger than HM vibrational modes, but the IR excitation field's $\delta\omega/\omega$ is also substantially narrower, which helps to selectively and resonantly generate the desired coherences while suppressing any SF contribution. Common sources of high intensity, sub-ps THz pulses (organic emitters, LiNbO3, etc) all have $\delta\omega \approx \omega$ and thus both Res and SF pathways must be considered when analyzing responses in the overlapping pump field region. Finally, we would like to note that our conclusions regarding the excitation mechanism of intra-molecular vibrational modes of HMs in 2D-TTR spectroscopy likely do not alter analyses performed on similar systems in the complementary 2D-TRT and 2D-RTT experiments.[12] Those measurements attributed spectral features that remained post-deconvolution to couplings between a Raman-excited vibrational coherence and a resonant one-quanta interaction

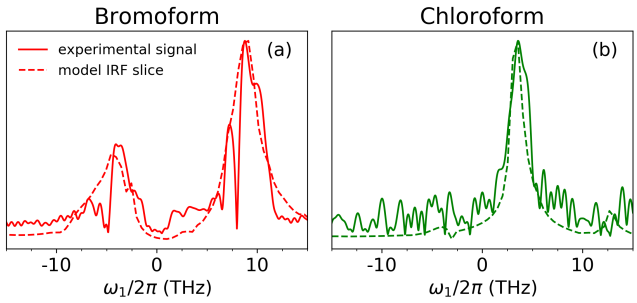

Figure 5: (a) Slices along ω_1 at ω_2=eigenmode of the IRF/RDM model and experimental response demonstrate the quality of fit for the bromoform data. Chloroform (b) is reproduced by slicing along the same IRF/SF-RDM model as shown in (a) at $\omega_2/2\pi$=7.8 THz, instead of at bromoform's $\omega_2/2\pi$=4.7 THz.

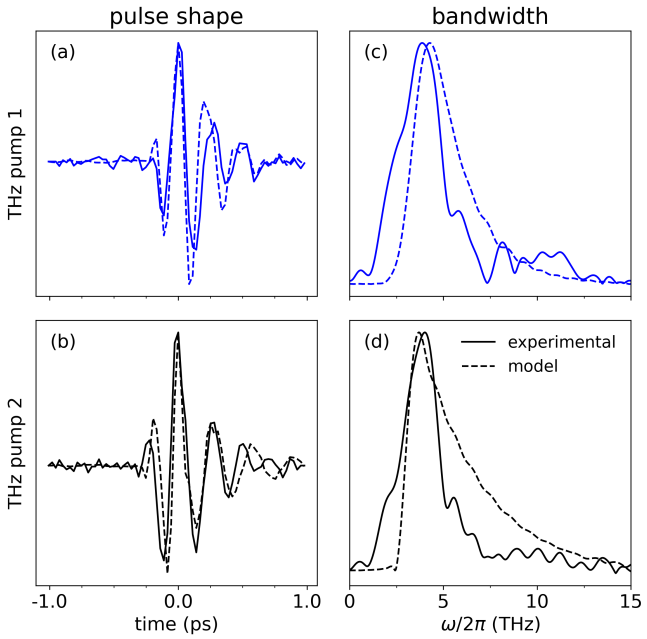

Figure 6: Comparison of the experimental and model THz pulse shapes (a,b) and corresponding bandwidths (c,d). See the SI for more detail on the optimization process used to obtain the model pulse shapes.

with bath modes of the liquid. Our conclusions are consistent with their observation that the IRF strongly determines the observed multi-dimensional experimental response.

In this work we provide extensive new experimental data and theoretical modeling that leads to a simple reinterpretation of previous 2D-TTR measurements of HMs. With this new analysis, we explain the complex 2D data sets for both bromoform and chloroform through a convolution of the experiment's THz fields with the molecules' intra-molecular vibrational modes. No coherence pathways outside of the SF-TKE process in Fig. 2 are required. The new analysis is also fully consistent with the observed magnitudes of transition dipole moments and molecular polarizabilities.

Moving forward, there are two keys lessons. First, large transition dipoles are crucial for performing truly resonant 2D-TTR experiments. Halogenated methanes unfortunately do not satisfy this requirement, and the bright, complex signals observed can easily be misattributed to resonant processes. Second, nearly transform-limited half-cycle THz fields would maximize the field strengths achievable, greatly simplify the experimental IRF structure, and reduce ambiguities in the analysis of dynamics in molecular systems.

References

(1) Mcmorrow, D.; Lotshaw, W. T.; Kenney-Wallace, G. A. Femtosecond Optical Kerr Studies on the Origin of the Nonlinear Responses in Simple Liquids. *IEEE Journal of Quantum Electronics* **1988**, *24*, 443–454.

(2) Cho, M.; Du, M.; Scherer, N. F.; Fleming, G. R.; Mukamel, S. Off-resonant transient birefringence in liquids. *Journal of Chemical Physics* **1993**, *99*, 2410.

(3) Tokmakoff, A.; Lang, M.; Larsen, D.; Fleming, G.; Chernyak, V.; Mukamel, S. Two-Dimensional Raman Spectroscopy of Vibrational Interactions in Liquids. *Phys. Rev. Lett.* **1997**, *79*, 2702–2705.

(4) Blank, D. A.; Kaufman, L. J.; Fleming, G. R. Fifth-order two-dimensional Raman spectra of CS2 are dominated by third-order cascades. *Journal of Chemical Physics* **1999**, *111*, 3105–3114.

(5) Kubarych, K. J.; Milne, C. J.; Lin, S.; Astinov, V.; Miller, R. J. D. Diffractive optics-based six-wave mixing: Heterodyne detection of the full chi((5)) tensor of liquid CS2. *Journal of Chemical Physics* **2002**, *116*, 2016–2042.

(6) Tanimura, Y.; Mukamel, S. Two-dimensional femtosecond vibrational spectroscopy of liquids. *The Journal of Chemical Physics* **1993**, *99*, 9496–9511.

(7) Hattori, T. Classical theory of two-dimensional time-domain terahertz spectroscopy. *Journal of Chemical Physics* **2010**, *133*.

(8) Ikeda, T.; Ito, H.; Tanimura, Y. Analysis of 2D THz-Raman spectroscopy using a

non-Markovian Brownian oscillator model with nonlinear system-bath interactions Analysis of 2D THz-Raman spectroscopy using a non-Markovian Brownian oscillator model with nonlinear system-bath interactions. **2015**, *212421*, 0–15.

(9) Savolainen, J.; Ahmed, S.; Hamm, P. Two-dimensional Raman-terahertz spectroscopy of water. *Proc. Natl. Acad. Sci. U. S. A.* **2013**, *110*, 20402–20407.

(10) Shalit, A.; Ahmed, S.; Savolainen, J.; Hamm, P. Terahertz echoes reveal the inhomogeneity of aqueous salt solutions. *Nat. Chem.* **2017**, *9*, 273.

(11) Hamm, P.; Shalit, A. Perspective: Echoes in 2D-Raman-THz spectroscopy. *J. Chem. Phys.* **2017**, *146*, 130901.

(12) Ciardi, G.; Berger, A.; Hamm, P.; Shalit, A. Signatures of Intra- And Intermolecular Vibrational Coupling in Halogenated Liquids Revealed by Two-Dimensional Raman-Terahertz Spectroscopy. *Journal of Physical Chemistry Letters* **2019**, *10*, 4463–4468.

(13) Allodi, M. A.; Finneran, I. A.; Blake, G. A. Nonlinear terahertz coherent excitation of vibrational modes of liquids. *Journal of Chemical Physics* **2015**, *143*, 234204.

(14) Finneran, I. A.; Welsch, R.; Allodi, M. A.; Miller III, T. F.; Blake, G. A. Coherent two-dimensional terahertz-terahertz-Raman spectroscopy. *Proceedings of the National Academy of Sciences* **2016**, *113*, 6857–6861.

(15) Finneran, I. A.; Welsch, R.; Allodi, M. A.; Miller, T. F.; Blake, G. A. 2D THz-THz-Raman Photon-Echo Spectroscopy of Molecular Vibrations in Liquid Bromoform. *Journal of Physical Chemistry Letters* **2017**, *8*, 4640–4644.

(16) Magdău, I. B.; Mead, G. J.; Blake, G. A.; Miller, T. F. Interpretation of the THz-THz-Raman Spectrum of Bromoform. *The Journal of Physical Chemistry A* **2019**, acs.jpca.9b05165.

(17) Mead, G.; Katayama, I.; Takeda, J.; Blake, G. A. An echelon-based single shot optical and terahertz Kerr effect spectrometer. *Review of Scientific Instruments* **2019**, *90*, 053107.

(18) Maehrlein, S.; Paarmann, A.; Wolf, M.; Kampfrath, T. Terahertz Sum-Frequency Excitation of a Raman-Active Phonon. *Physical Review Letters* **2017**, *119*, 1–6.

(19) Juraschek, D. M.; Maehrlein, S. F. Sum-frequency ionic Raman scattering. *Physical Review B* **2018**, *97*, 1–8.

(20) Shishkov, V. Y.; Andrianov, E. S.; Pukhov, A. A.; Vinogradov, A. P.; Lisyansky, A. A. Enhancement of the Raman Effect by Infrared Pumping. *Physical Review Letters* **2019**, *122*, 153905.

(21) Sidler, D.; Hamm, P. Feynman diagram description of 2D-Raman-THz spectroscopy applied to water. *Journal of Chemical Physics* **2019**, *150*.

(22) NIST Mass Spectrometry Data Center, d., William E. Wallace *NIST Chemistry WebBook, NIST Standard Reference Database 69*; National Institute of Standards and Technology, 1997; type: dataset.

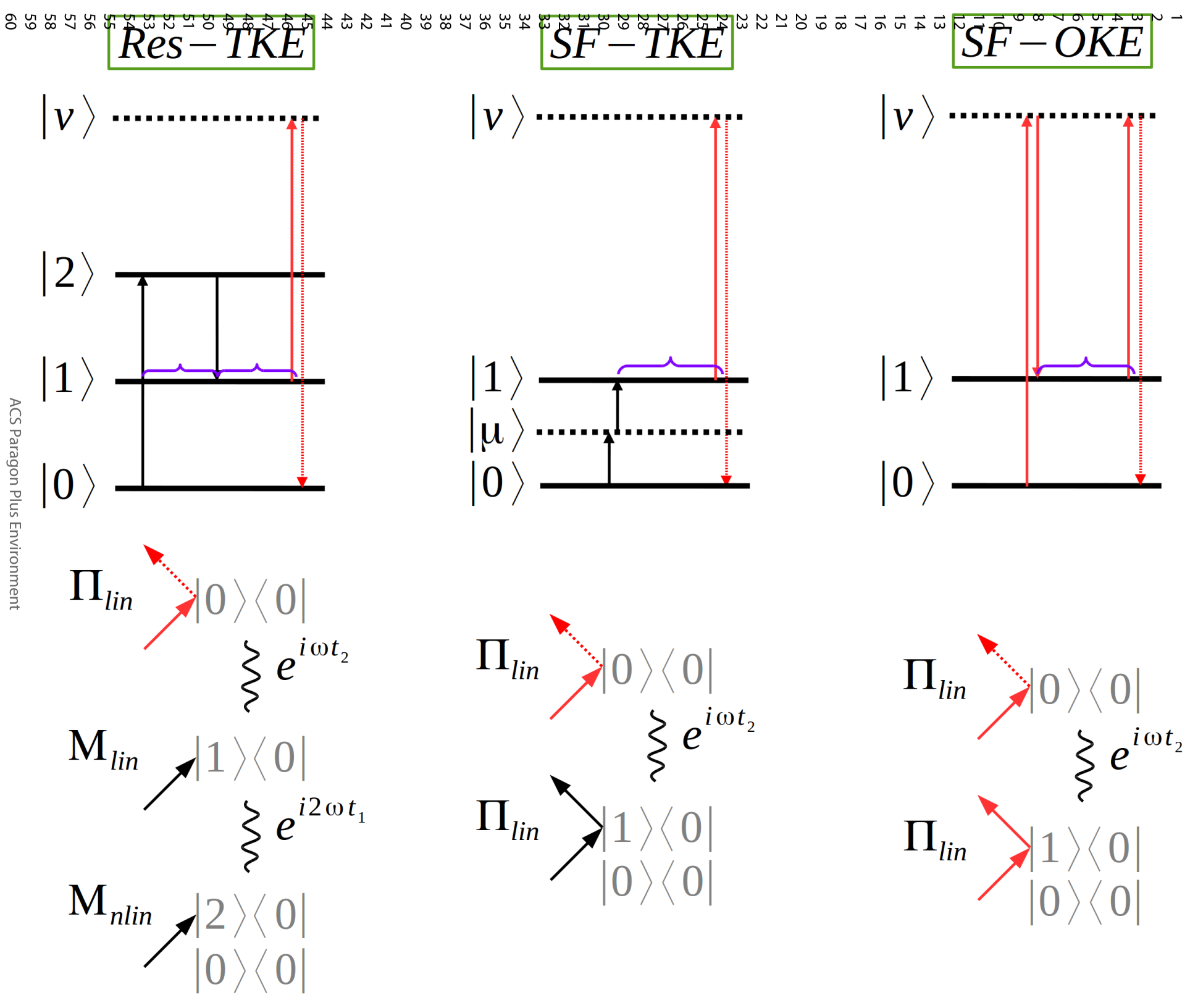
Res − TKE
SF − TKE
SF − OKE
|ν⟩
|2⟩
|1⟩
|μ⟩
|0⟩
Π_lin
|0⟩⟨0|
e^{iωt_2}
M_lin
|1⟩⟨0|
e^{i2ωt_1}
M_nlin
|2⟩⟨0|
|0⟩⟨0|
Π_lin
|0⟩⟨0|
e^{iωt_2}
Π_lin
|1⟩⟨0|
|0⟩⟨0|
Π_lin
|0⟩⟨0|
e^{iωt_2}
Π_lin
|1⟩⟨0|
|0⟩⟨0|

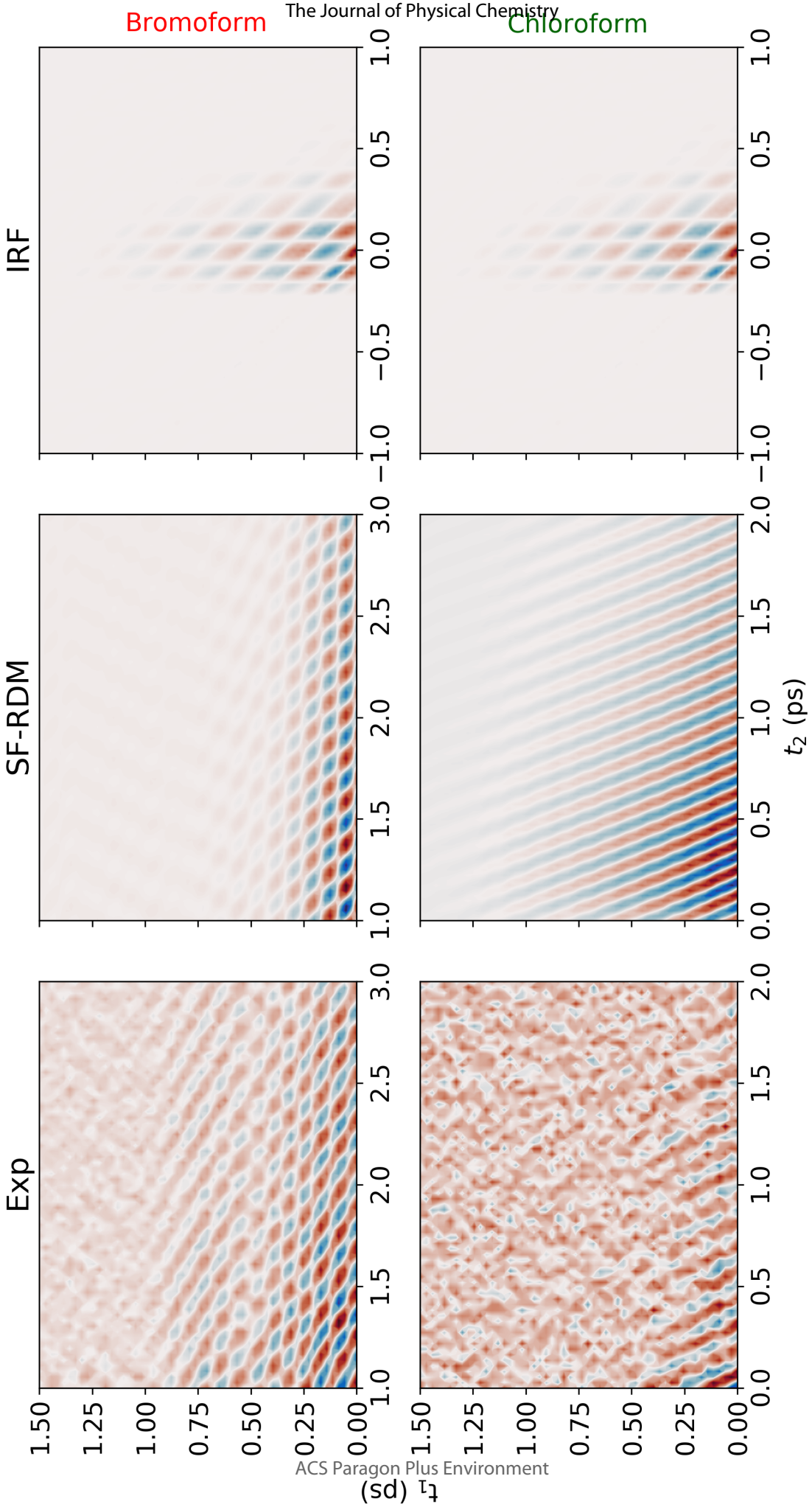
Bromoform
Chloroform
IRF
SF-RDM
Exp
t_2 (ps)
t_1 (ps)

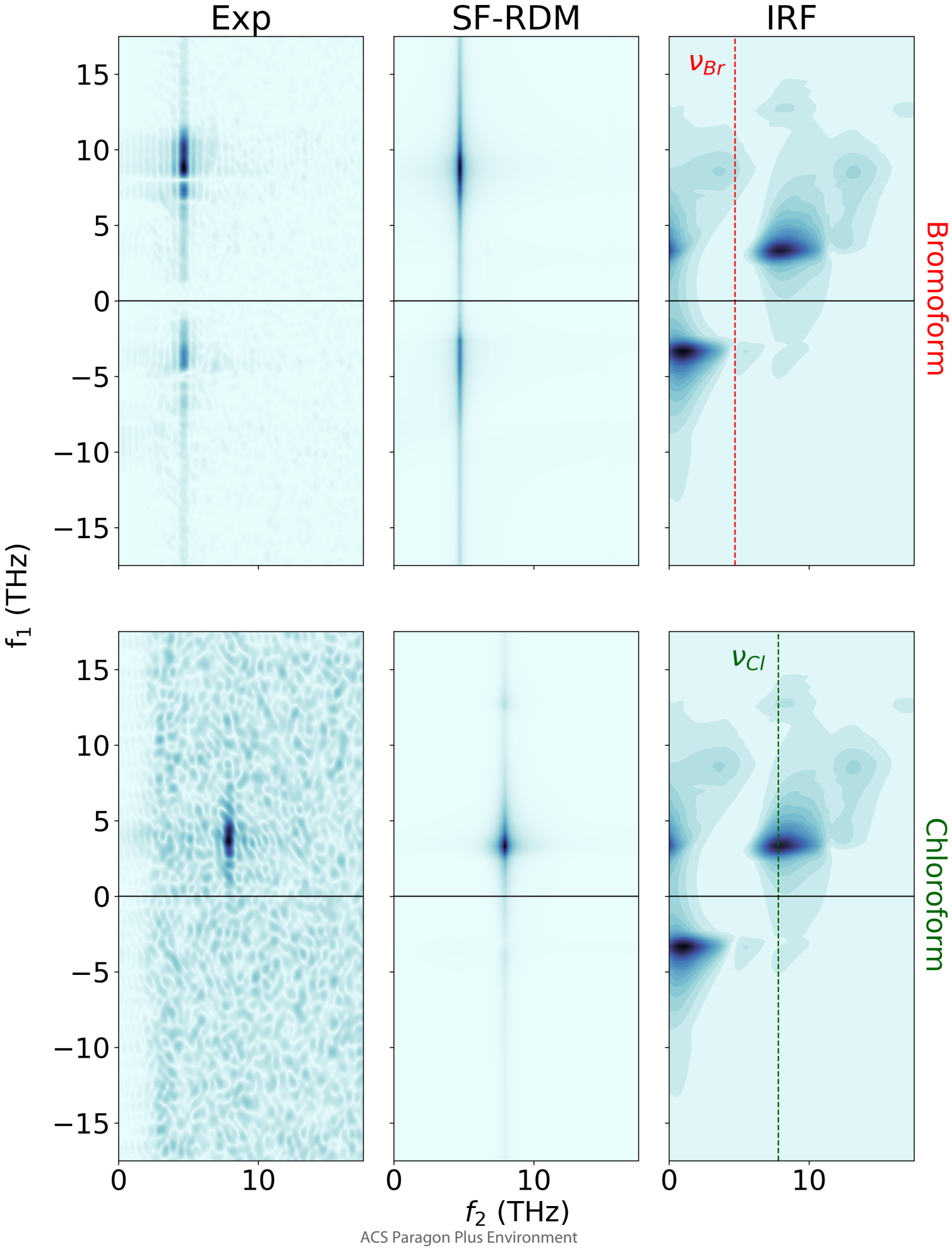
Exp
SF-RDM
IRF
ν_{Br}
ν_{Cl}
Bromoform
Chloroform
f_1 (THz)
f_2 (THz)
15
10
5
0
−5
−10
−15
0
10

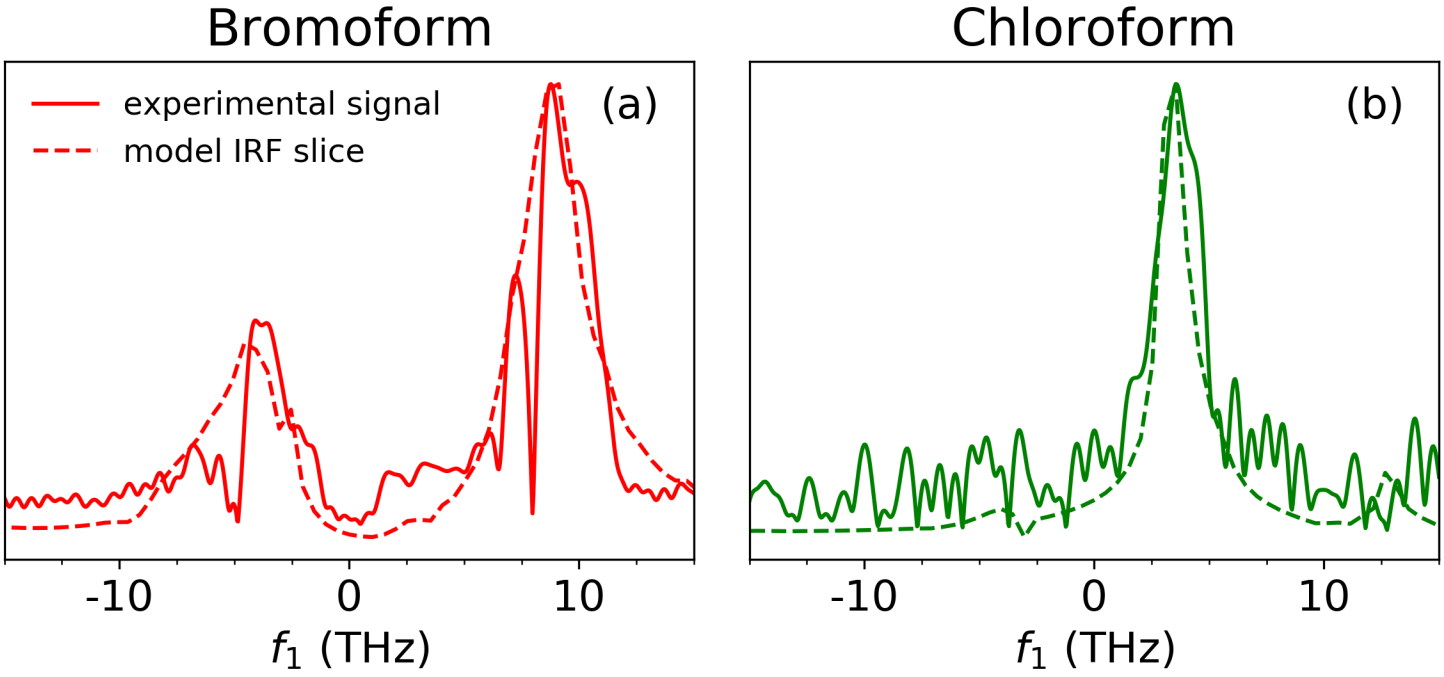
Bromoform
Chloroform
experimental signal
model IRF slice
(a)
(b)
-10
0
10
f_1 (THz)

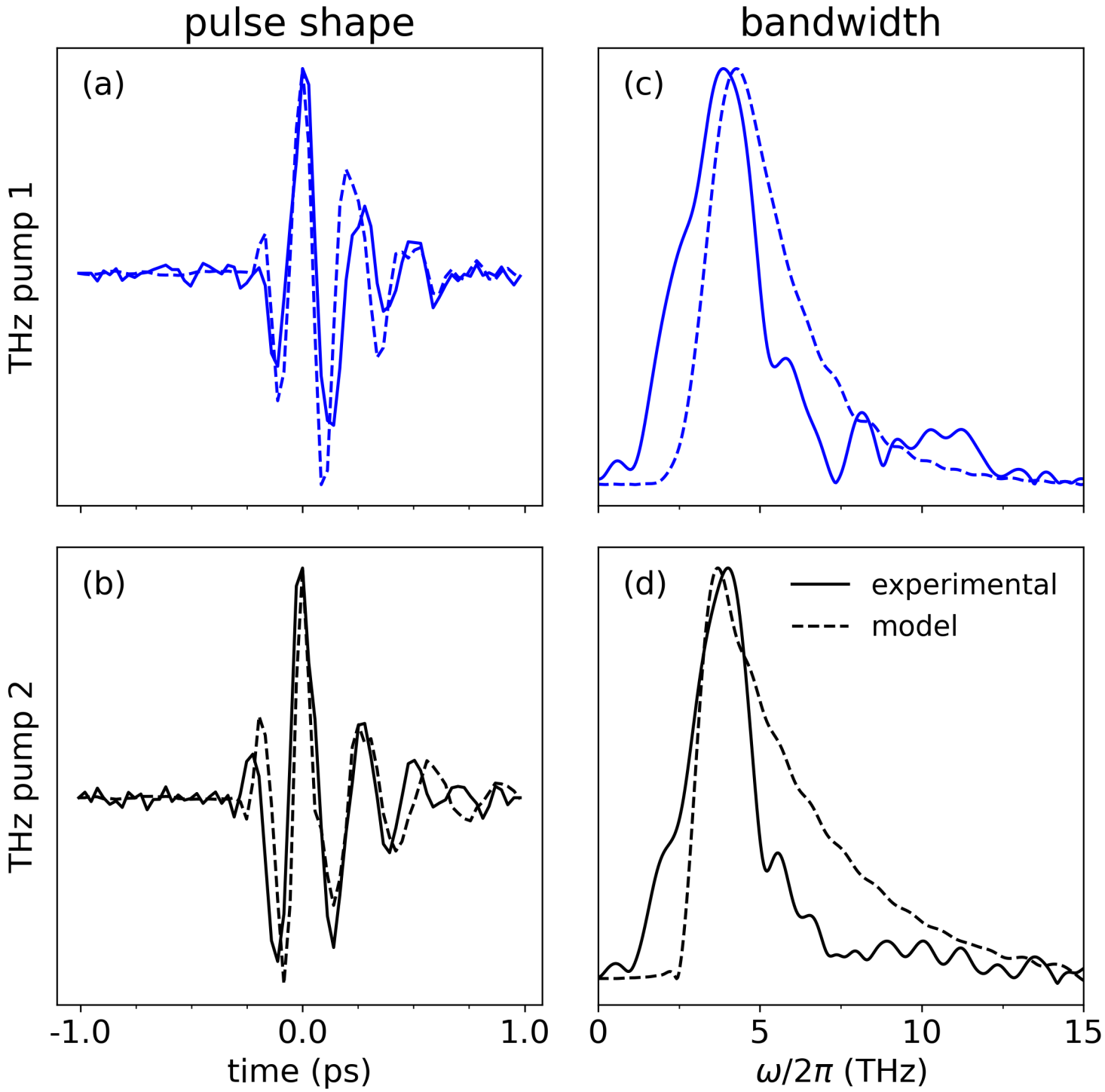
pulse shape
bandwidth
(a)
(c)
(b)
(d)
THz pump 1
THz pump 2
experimental
model
-1.0
0.0
1.0
time (ps)
0
5
10
15
ω/2π (THz)